BEAM DYNAMICS

https://doi.org/10.46813/2021-133-045

MULTI-PURPOSE MODES OF FORMATION OF ELECTRON BEAMS IN THE CYLINDRICAL MAGNETIC FIELD OF THE MAGNETRON GUN

A.S. Mazmanishvili, N.G. Reshetnyak
National Science Center "Kharkov Institute of Physics and Technology", Kharkiv, Ukraine
E-mail: nreshetnyak@kipt.kharkov.ua

The results of the study on the formation of electron beams by the magnetron gun at various configurations of the magnetic field in the beam transport channel are presented. A technique for modeling the processes of formation of electron flows and control of the distribution of beams by collimation is presented. Numerical simulation of the dynamics of electron beams in the magnetic field of the gun for its various configurations has been carried out. Experimental data on the transportation and collimation of electron beams are presented. The possibility of stable formation of an electron beam in the axial direction during its transportation is shown. Imprints of the collimated electron beam were obtained on metal targets. The possibility of controlling the beam diameter by varying the magnetic field is shown. Comparison of the results of numerical modeling and experimental data on the motion and collimation of the tubular electron flow is carried out.

PASC: 29.17.+w

INTRODUCTION

The study of electron beams of various configurations and intensities is associated with their application in high-voltage pulsed microwave electronics, accelerator technology, etc. [1, 2]. Irradiation of targets with electron beams with specified parameters makes it possible to regulate the structural-phase state in the surface layers and change the properties of materials [1 - 5]. In practice, beam technologies for material processing are being introduced into industrial production. To solve these problems, accelerators of intense electron beams with an electron energy of 100…400 keV are used [1, 3]. A linear electron accelerator for irradiation of metal targets has been created at the NSC KIPT [4]. One of the main elements of the accelerator is the magnetron gun with cold metal cathodes. Irradiation of various metal targets was carried out [5] and the possibility of irradiating the inner cylindrical surface using the tubular electron beam was studied [6].

This paper describes the results of an experimental study of the modes of irradiation with the collimated electron beam of metal targets located at selected distances. Multipurpose mode is used with collimation. Imprints of the collimated electron beam on metal targets are shown.

ELECTRON TRAJECTORIES SIMULATION TECHNIQUE

Let the electron with energy E, moving parallel (or at the angle) to the axis at some distance r_0 from it, flies into the magnetic field. It is required to construct the equation of motion of particle in the magnetic field and, based on the solution of the equation of motion for the selected moments of time t, determine the coordinates of the electron.

To construct the mathematical model of the solution, we will use the axial symmetry of the problem and work in a polar coordinate system (r, z, ϑ). In it, the Hamiltonian has the form

$$H = \frac{p_r^2 + p_z^2}{2m} + \frac{1}{2m}\left(\frac{p_\vartheta}{r} - e_0 A\right)^2, \qquad (1)$$

where e_0, m – charge and rest mass of the electron; p_r, p_z, p_ϑ – canonical impulses; A – magnetic potential. The equations of motion for coordinates and impulses have the form of a system $\dot{r} = \partial H / \partial p_r$, $\dot{z} = \partial H / \partial p_z$, $\dot{\vartheta} = \partial H / \partial p_\vartheta$, $\dot{p}_r = -\partial H / \partial r$, $\dot{p}_z = -\partial H / \partial z$, $\dot{p}_\vartheta = -\partial H / \partial \vartheta$. In it, we pass, using the speed of light c, from the current time t to the variable $s = ct$, the derivative of which will be denoted by a prime. For impulses, we will replace $p_r = e_0 B q_r$, $p_z = e_0 B q_z$, $p_\vartheta = e_0 B q_\vartheta$. As a result, we arrive at the system of equations

$$\begin{cases} r' = \mu q_r, \\ z' = \mu q_z, \\ \vartheta' = \mu\left(q_\vartheta / r^2 - f(z)\right), \\ q_r' = \mu r\left(q_\vartheta / r^2 - f(z)\right)\left(q_\vartheta / r^2 + f(z)\right), \\ q_z' = \mu r^2\left(q_\vartheta / r^2 - f(z)\right) df(z)/dz, \\ q_\vartheta' = 0. \end{cases} \qquad (2)$$

In them: $\mu = e_0 B / mc$; B – the magnetic field strength at the point under consideration z; $Bf(z)$ – the function describing the magnetic field strength along the axis z; $df(z)/dz$ – the analytical derivative of the function $f(z)$. These quantities are related to the magnetic potential of the field, which, taking into account the azimuthal symmetry, is written in the form $A(r,z) = Brf(z)$. The method for obtaining the field function of the longitudinal coordinate $f(z)$ based on the data of the initial magnetic field is described in [6, 7]. Equations (2) must be supplemented with the initial conditions for r_0, z_0, ϑ_0, and also for q_{r0}, q_{z0}, $q_{\vartheta 0}$.

So, from a computational point of view, the problem can be formulated as the problem of finding a solution to a system of ordinary differential equations with given initial conditions. The formulated problem can be solved, provided that it is possible at each step of integration of equations (2) to use functions $f(z)$ and $df(z)/dz$ as analytical functions.

In Fig. 1 block diagram of the setup is shown on which experimental studies on the formation of electron beams and measurement of their characteristics in the electron beam transport channel were carried out.

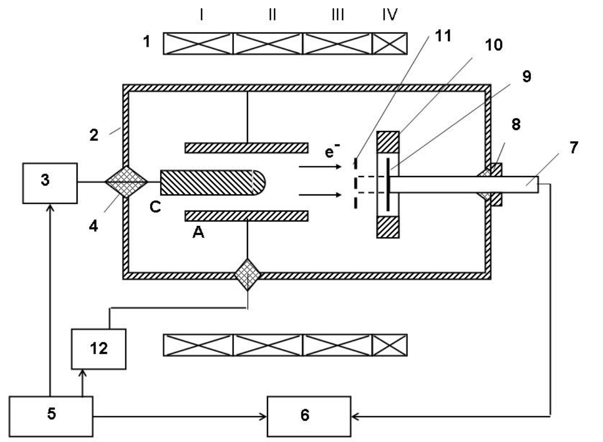

Fig. 1. Experimental setup:
1 – solenoid sections (I, II, III, IV); 2 – vacuum volume; 3 – high-voltage generator; 4 – insulator; 5 – synchronization unit; 6 – measuring system; 7 – centering rod; 8 – seal; 9 – cylinder Faraday (metal target); 10 – ring magnet; 11 – replaceable collimator; 12 – generator; A – anode; C – cathode

MAIN RESULTS

The magnetic field was created by the H_S solenoid and the solenoid together with the H_{SM} permanent magnet. The experiments were carried out with the magnetron gun (cathode diameter 36 mm, length 75 mm, anode inner diameter 78 mm, length 135 mm) at a cathode voltage of 20...80 kV. Three-sector and 8-point collimation of electron beams was used in the work.

In 3-sector collimation, the beam prints were recorded using two targets located at distances $z = 150$ mm and $z = 210$ mm. The results of the study were recorded on metal targets, which made it possible to interpret the dynamics of electron beams.

In Fig. 2 for a magnetic field with a maximum amplitude of 0.41 T shows: calculated dependences of the sector distribution of the electron beam (sample size 600 particles, graduation 12 mm/div).

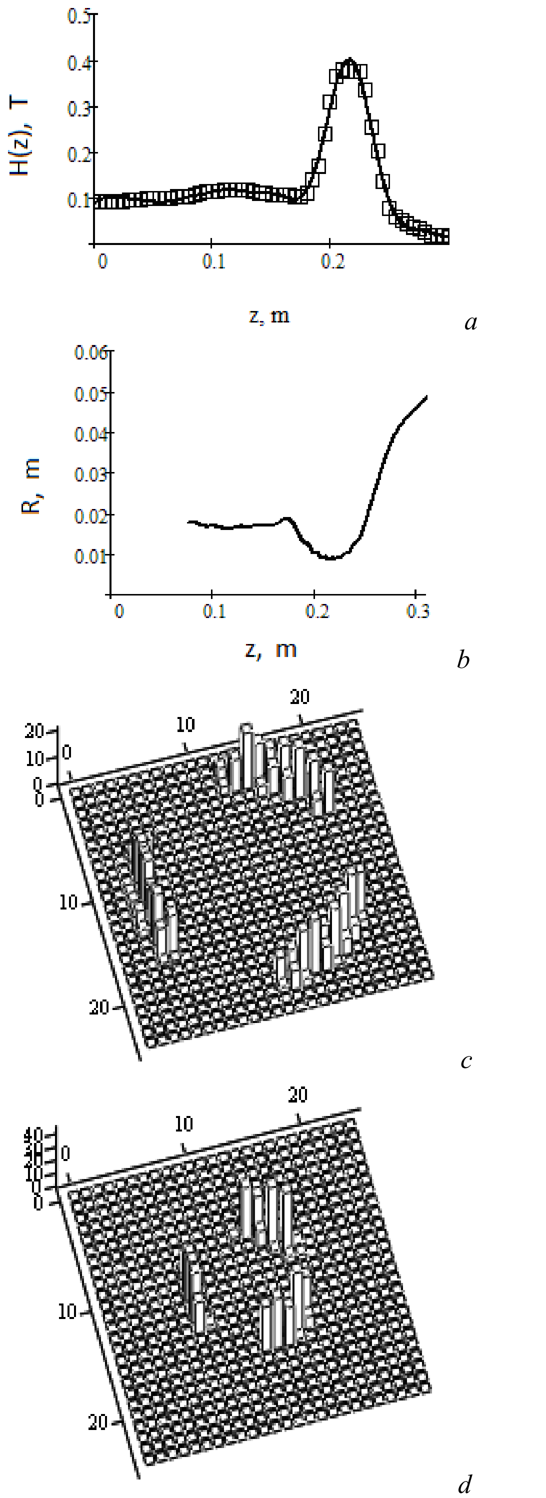

Fig. 2. Characteristics of the sectorial electron flow: the amplitude H_{SM} of the gradient magnetic field (squares are the experimental data) (a); the dependence of the average beam radius R on the coordinate z (b); the calculated beam distribution after the sector collimator (z=75 mm) (c); the calculated distribution of particles (z=210 mm) (d)

Fig. 3,b,c were obtained using the three-sector collimator.

In Fig. 3,a shows the imprint of the beam at the distance $z = 150$ mm in a uniform magnetic field (see Fig. 2) with an amplitude of 0.11 T.

In Fig. 3,b shows the sectorial imprint of the beam obtained under the same conditions as in Fig. 3,a. When the electron beam moves in an increasing magnetic field with an amplitude of 0.35 T (z = 210 mm), the beam is focused. The outer diameter of the beam D decreases from 40 to 24 mm.

In Fig. 3,c shows the imprint of the beam in the magnetic field at the distance of z = 210 mm.

In Figs. 2 and 3, one can see the decrease in the beam size in the region of the maximum amplitude of the H_{SM} magnetic field. It was found that with the increase in the maximum field amplitude, the effect of radial compression of the beam is more pronounced.

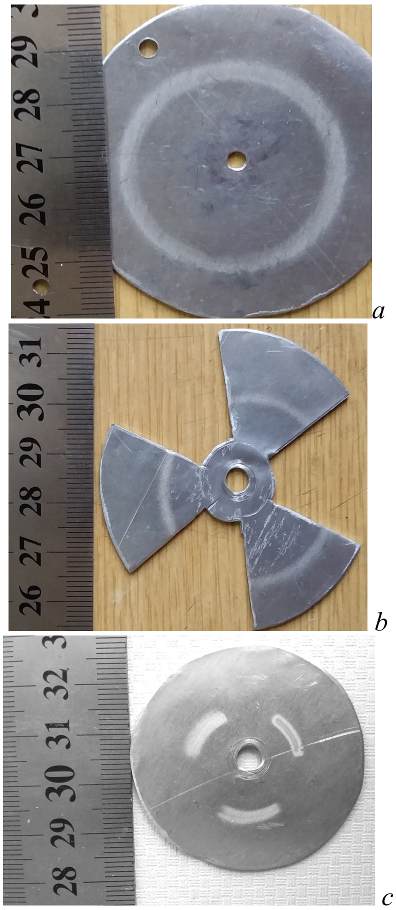

Fig. 3. Imprints of beam on targets:
without collimator (a);
on the collimator (z=150 mm) (b);
after the collimator (z=210 mm) (c)

Experiments were carried out with a magnetron gun with the 8-beam electron flow in decreasing and increasing magnetic fields. To obtain the imprint of the beam, two targets were used, which were placed at distances z = 210 mm and z = 270 mm.

For the solenoidal magnetic field H_S with the maximum amplitude of 0.15 T, the calculated dependences (two-dimensional histograms at z = 75 mm and z = 270 mm, scale division 12 mm/div) of 8 beam distributions of beam particles (sample size 600 particles) and imprints of the beam in the target plane in the region of the field decay (z = 270 mm) are shown in Fig. 4.

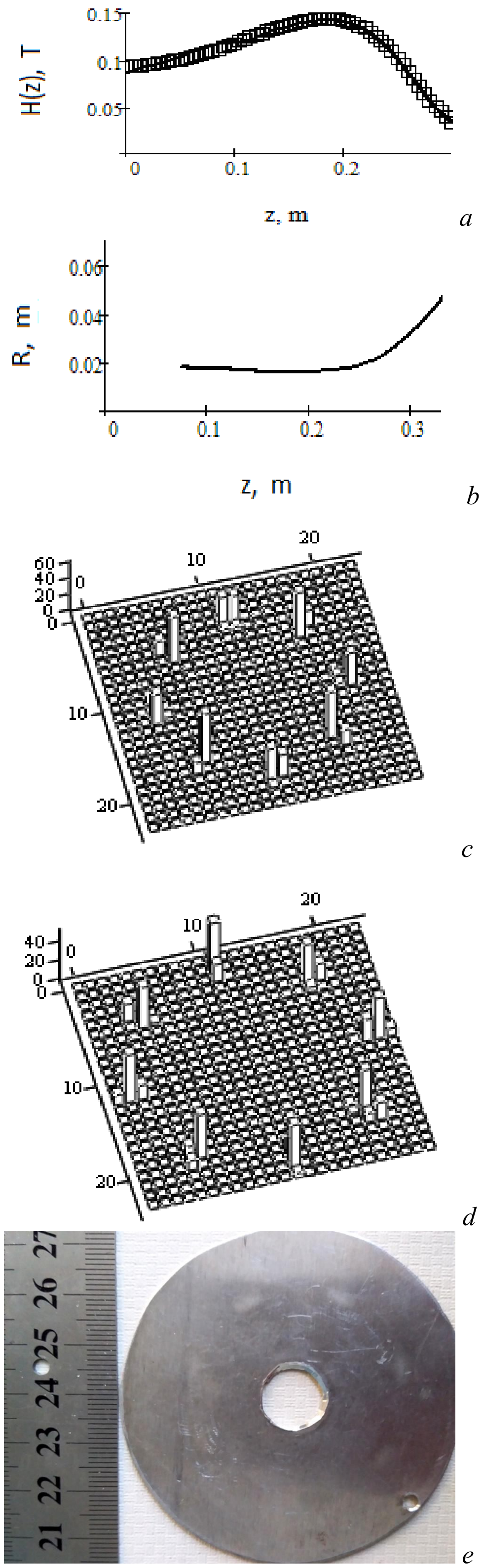

Fig. 4. Characteristics of 8-beam electron flow:
the amplitude $H_S(z)$ of the magnetic field (a);
the dependence of the beam radius R on the longitudinal coordinate z (b); the beam distribution histogram at the start (z=75 mm) (c); the calculated particle distribution (z=270 mm) (d); the imprint beam on the target (z=270 mm) (e)

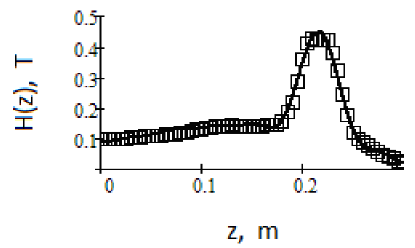

a

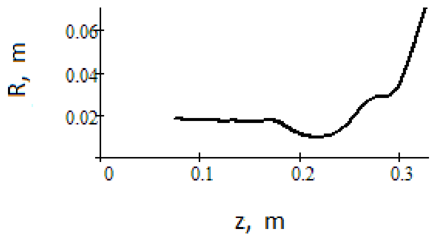

b

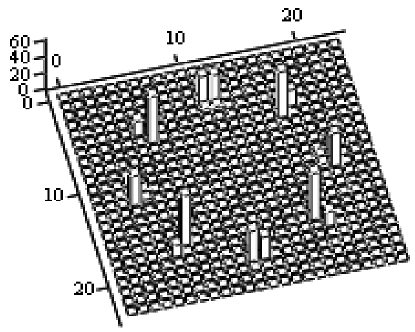

c

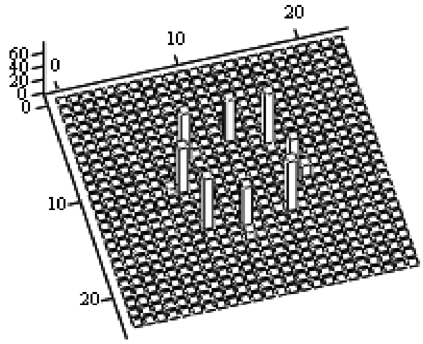

d

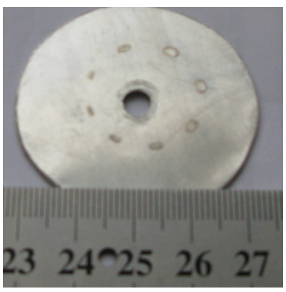

e

Fig. 5. Characteristics of 8-beam electron flow: the amplitude $H_{SM}(z)$ of the gradient magnetic field (a); the dependence of the average beam radius R on the longitudinal coordinate z (b); the beam distribution at the start (z=75 mm) (c); the calculated distribution of particles (z=210 mm) (d); beam imprint on the target (z=210 mm) (e)

From the Fig. 4 one can see the increase in the beam size with the decrease in the amplitude of the magnetic field. When the electron beam moves, the outer diameter of the beam D in the decreasing magnetic field with the gradient of 0.01 T/cm and the amplitude of 0.07 T on the target at the cathode voltage of 60 kV was 44 mm.

In Fig. 5 for the H_{SM} magnetic field with the maximum amplitude of 0.41 T, the following are similarly presented: calculated dependences (two-dimensional histograms at z = 75 mm and z = 210 mm, scale division 12 mm/div) of 8 beam distributions of the electron flow (sample size 600 particles) and beam imprints in the target plane in the region of increasing field (z = 210 mm). When the electron beam moves in an increasing magnetic field with a gradient of 0.1 T/cm and an amplitude of 0.41 T, the outer beam diameter D decreases from 40 to 22 mm.

In Fig. 5 one can see the focusing effect of a decrease in the beam size with an increase in the maximum amplitude of the magnetic field.

CONCLUSIONS

The prints of collimated electron beams on metal targets located at various selected distances were obtained experimentally. The solution to the direct problem of modeling the trajectories of electrons for given conditions is found. Based on the algorithm for finding the magnetic field amplitude $H(z)$ along the solenoid axis and the derivative $dH(z)/dz$ as *analytical* functions of the longitudinal coordinate z, the magnetic field distribution is reconstructed. The calculated dependences of the particle beam distribution in the target plane are presented. The possibility of stable regulation of the beam diameter by varying the magnetic field is shown. Comparison of the results of numerical modeling and experimental data on the motion and collimation of the tubular electron flow is carried out.

On the basis of the constructed software, the number of inverse problems can be considered, including those whose purpose is to find the parameters of the system and the operating mode to obtain the beam distribution at the given place and with given properties.

REFERENCES

1. V.I. Engelko, G. Mueller, A. Andreev, et al. Pulsed Electron Beam Facilities (GESA) for Surface Treatment // *Proc. of 10th International Conf. on Applied Charged Particle Accelerators in Medicine and Industry*. St.-Petersburg, Russia. 2001, p. 412-417.
2. I.V. Barsuk, G.S. Vorobiev, A.A. Ponomareva. Numerical modeling of the processes of formation of electron beams in axially symmetric systems // *Journal Nano- and Electronic Physics*. 2014, v. 6, № 2, p. 02012-1.
3. M.F. Vorogushin, V.A. Glukhikh, G.S. Manukyan, et al. Beam and ion-plasma technologies // *Problems of Atomic Science and Technology. Series "Physics of Radiation Effects and Radiation Materials Science"*. 2002, № 3, p. 101-109.
4. A.N. Dovbnya, V.V. Zakutin, N.G. Reshetnyak, et al. Studies of beam formation in the electron accelerator with a secondary-emission source // *Visnyk KhNU. Series "Nuclei, Particles Fields"*. 2006, № 732 2(30), p. 96-100.
5. A.N. Dovbnya, S.D. Lavrinenko, V.V. Zakutin, et al. Surface modification of zirconium and Zr1%Nb alloy by the electron beam of the magnetron gun-

based accelerator // *Problems of Atomic Science and Technology. Series "Physics of Radiation Effects and Radiation Materials Science"*. 2011, № 2, p. 39-45.
6. N.I. Ayzatsky, A.N. Dovbnya, A.C. Mazmanishvili, N.G. Reshetnyak, V.P. Romas'ko, I.A. Chertishchev. Studies on formation of the radially-directed electron beam generated by the magnetron gun with a secondary emission cathode // *Problems of Atomic Science and Technology. Series "Nuclear Physics Investigations"*. 2016, № 3, p. 11-18.
7. A.S. Mazmanishvili, N.G. Reshetnyak. Transformation of the data array of the cylindrical magnetic field of the magnetron gun and the problem of the radial motion of electrons // *Applied Problems of Mathematical Modeling*. 2020, v. 3, № 1, p. 108-116.

Article received 20.04.2021

МНОГОЦЕЛЕВЫЕ РЕЖИМЫ ФОРМИРОВАНИЯ ЭЛЕКТРОННЫХ ПУЧКОВ В ЦИЛИНДРИЧЕСКОМ МАГНИТНОМ ПОЛЕ МАГНЕТРОННОЙ ПУШКИ

А.С. Мазманишвили, Н.Г. Решетняк

Представлены результаты исследования по формированию магнетронной пушкой электронных пучков при различных конфигурациях магнитного поля в канале транспортировки пучка. Изложены методика моделирования процессов формирования электронных потоков и управления распределения пучков коллимирования. Проведено численное моделирование динамики электронных пучков в магнитном поле пушки при различных его конфигурациях. Приведены экспериментальные данные по транспортировке и коллимированию электронных пучков. Показана возможность устойчивого формирования электронного пучка в осевом направлении при его транспортировке. Получены отпечатки коллимированного электронного пучка на металлических мишенях. Показана возможность регулирования диаметра пучка путем вариации магнитного поля. Проведено сравнение результатов численного моделирования и опытных данных по движению и коллимации трубчатого электронного потока.

БАГАТОЦІЛЬОВІ РЕЖИМИ ФОРМУВАННЯ ЕЛЕКТРОННИХ ПУЧКІВ У ЦИЛІНДРИЧНОМУ МАГНІТНОМУ ПОЛІ МАГНЕТРОННОЇ ГАРМАТИ

О.С. Мазманішвілі, М.Г. Решетняк

Представлено результати дослідження щодо формування магнетронною гарматою електронних пучків при різних конфігураціях магнітного поля в каналі транспортування пучка. Викладена методика моделювання процесів формування електронних потоків і управління розподілом пучків методом колімування. Проведено чисельне моделювання динаміки електронних пучків у магнітному полі гармати при різних його конфігураціях. Наведено експериментальні дані з транспортування і колімування електронних пучків. Показана можливість стійкого формування електронного пучка в осьовому напрямку при його транспортуванні. Отримано відбитки колімованого електронного пучка на металевих мішенях. Показана можливість регулювання діаметра пучка шляхом варіації магнітного поля. Проведено порівняння результатів чисельного моделювання і дослідних даних по руху і колімації трубчастого електронного потоку.